

A Multi-Pronged Approach to Assessing Inflammatory Inhibitory Activity of a New Cyclic Alkaloid Compound from Root Bark of *Ziziphus Nummularia* (Aubrev.)

Sarbani Dey Ray

Assam University - Dargakona Campus: Assam University

Nirupam Das

Assam University - Dargakona Campus: Assam University

Supratim Ray (✉ supratimray75@gmail.com)

Assam University - Dargakona Campus: Assam University <https://orcid.org/0000-0002-3570-2040>

Research Article

Keywords: Ziziphus nummularia, IC, NO, TNF- α , ADME, molecular docking

Posted Date: December 20th, 2021

DOI: <https://doi.org/10.21203/rs.3.rs-1134126/v1>

License:   This work is licensed under a Creative Commons Attribution 4.0 International License.

[Read Full License](#)

Abstract

[(16-methoxy-10-(3-methyl-butyl)-2-oxa-6, 9, 12-triaza-tricyclo [13.3.1.03, 7] nonadeca-1(18), 13, 15 (19), 16-tetraene-8, 11-Dione], a putative cyclic alkaloid compound (IC) isolated from the root bark of *Ziziphus nummularia*, showed potential anti-inflammatory potential. Nitric oxide (NO), prostaglandin-E₂ (PGE₂), and tumour necrosis factor-alpha (TNF- α) levels were measured *in vitro* to assess IC's potential. ADME simulations and molecular docking of IC by TNF- α receptor were also performed. The *in vivo* potentials of IC and ethanolic extract (EE) were investigated by assessing carrageenan-induced paw oedema and arachidonic acid/xylene-induced ear oedema. TNF- α inhibition was higher in IC than in others, with a maximal percent inhibition of 88.00 percent at 50.11 μ M. IC generated hydrogen bonds with ASP 45 and GLN 47, according to *in silico* research. Carrageenan, xylene, and arachidonic acid-induced oedema were all significantly reduced by IC. As a result, IC may have clinical potential in the future treatment of inflammation.

1. Introduction

The inflammatory response is a complex immunopathological process [1]. As a result of the increased prevalence of this process, more cases of neoplasm are being discovered on a daily basis [2, 3]. The presence of extra mediators in macrophages caused this immunopathological response [4, 5]. There are two types of inflammatory mediators: pro and anti-mediators. Both qualities, however, are seen in interleukin (IL) [6]. One of the most significant cytokines is tumour necrosis factor (TNF- α). TNF- α has a wide range of biological effects and has been connected to a number of disorders [7, 8]. Nitric oxide, like TNF- α , is a pro-inflammatory mediator. Citrulline is created as a by-product of the arginine-to-NO conversion. NO has been linked to a number of inflammatory disorders affecting many parts of the body, including the joints, intestines, and lungs [9, 10]. As a result, a chemical that may reduce NO offers a substantial advancement in the treatment of inflammation. Prostaglandin-E₂ (PGE₂) is the most common cytokine, along with TNF- α and NO. It is in charge of a number of functions, including immune response modulation and blood pressure regulation, among others. Due to its considerable role in the process, PGE₂ shows the basic signs of inflammation, such as redness, swelling, and finally pain [11]. As a result, blocking these mediators, such as TNF- α , PGE₂, and NO production, is a research target for generating a novel chemical entity that can treat inflammation.

The Rhamnaceae family includes *Ziziphus nummularia* (Aubrev.). The plant thrives in India's semi-arid and dry regions. It is used to cure inflammation, cough, cold, diarrhoea, dysentery, and pain discomfort in the indigenous population [12–14]. Anti-inflammatory properties are found in the leaves of this plant, as well as those of other species in the same genus [15–17]. Leaf and fruit extracts have yielded a few molecules. The plant's root bark is used for a limited amount of work. A triterpene derivative extracted from the plant's root bark had previously been shown to have anticancer and anti-inflammatory properties by the current group [18–19].

To get a better knowledge of drug-receptor interactions, several *in silico* techniques have been used in rational drug design. Understanding the chemical mechanism via which newer drugs displayed anti-inflammatory properties is also critical. Molecular docking is one of the computational strategies that is gaining favour in computational drug design.

In light of the foregoing, the project's goal is to isolate, elucidate the structure, and investigate the mechanism of action of the isolated molecule (IC). The job was broken down into four sections. Initially, a new chemical entity was isolated and its structure was determined. Following that, *in vitro* activity was used to test the activity of the isolated compound. Following that, an *in silico* study was conducted to investigate the interaction of IC with a specific inflammatory mediator (in our example, TNF- α). Finally, *in vivo* investigations were carried out to see how IC affected an animal model (mice in our case). Furthermore, the *in vivo* potentials of ethanolic extract (EE) were measured and compared to that of IC.

2 Results

2.1 Isolation and structural elucidation

The fractions 49 to 56 from column exhibited one large spot with minor contamination throughout TLC silica plates after employing dragendorff reagent. Impurities were removed by hexane washing. The fractions (49-56) were blended and squeezed together. After that, it was cleaned with hexane once more. A total of 0.075g of product was created. The bioactive eluent was separated by HPTIC at 450 nm using solvent solutions of methanol, ethyl acetate, chloroform, and formic acid (1:7:2:0.2). The R_f value, height, and area were 0.59, 2.8, and 111, respectively (**Supplementary file: Figure S1**). The m.p is 465-468 °C. The elemental analysis (%) of the isolated compound (C₂₁H₂₉N₃O₄) is as follows (Calculated: C, 65.09; H, 7.54; N, 10.84; O, 16.52. Found: C, 65.17; H, 7.55; N, 10.86; O, 16.54).

The isolated compound showed following spectral characteristics. ¹HNMR (CDCl₃): δ 4.336 (d, $J=9.6$, H-3), 1.971 (d, $J=6.4$, H-4), 2.803 (s, H-5), 8.516 (d, H-6), 4.632 (d, $J=14.8$, H-7), 8.475 (s, H-9), 4.761 (d, $J=11.2$, H-10), 8.452 (s, H-12), 7.530 (t, $J=6.0$ Hz, H-13), 7.380 (d, $J=4.4$ Hz, H-14), 6.977 (d, $J=15.2$ Hz, H-15), 6.742, (d, $J=10.4$ HZ, H-17), 6.904 (d, $J=16.4$ Hz, H-18), 7.214 (s, $J=4.8$ Hz, H-19), 3.817 (s, $J=4.0$ Hz, H, of -OCH₃), 1.712 (s, H-10-1'), 1.298 (s, $J=4.0$, H-10-2'), 1.987(d, $J=6.4$, H-10-3'), 0.947 (d, $J=13.6$ Hz, H-10-4') (**Supplementary file: Figure S2 to S5**).

¹³CNMR (CDCl₃): δ 150.240 (-CH=, C-1 / 16), 77.017 (CH-, C-3), 39.176 (CH₂-, C-4 / 5), 171.196 (-C=O, C-8 / 11), 55.874 (-CH-, C-10), 32.432 (CH₂-, C-10-1', 10-2'), 29.706 (CH- C-10-3'), 14.771(-CH₃, C-10-4'), 118.17 (CH=, C-13 / 14), 128.766 (CH- C-15), 60.369 (-OCH₃, O-CH₃), 113.674 (CH-, C-17 / 18 / 19), (**Supplementary file: Figure S6**).

IR (KBr) ν_{\max} 2955, 2869, 1686, 1648, 3065, 3394, 1221, 1033, 883, 1454, 1376 cm⁻¹ (**Supplementary file: Figure S7**)

MS (FAB; m/z): 387. [M+1]; (**Supplementary file: Figure S8**). The orbitrap high-resolution MS showed the mass of isolated compound is 378.4711 (**Supplementary file: Figure S9**). The structure of isolated compound (**IC**) was given in Figure 1. To the best of our knowledge this is the first-time reporting of the isolated compound, i.e., [(16-methoxy-10-(3-methyl-butyl)-2-oxa-6, 9, 12-triaza-tricyclo [13.3.1.0^{3,7}] nonadeca-1(18), 13, 15 (19), 16-tetraene-8, 11-dione] from this species.

2.2 *In vitro* work

2.2.1 Effect of IC on NO, PGE₂ and TNF- α production

After cells (RAW 264.7) were treated with LPS/IFN- γ , increases in NO, TNF- α , and PGE₂ were found, as shown in Figure 2. The effect of IC on NO production was dose-dependent, with the highest percent inhibition being 67.00 percent at 50118.72 nM (~50.11 μ M). PGE₂ inhibition, on the other hand, does not appear to be dose-dependent, with the maximum inhibition of 55.00 percent occurring at 100 nM. IC also had a concentration-dependent effect on TNF- α production. The highest percent inhibition was 88.00 percent at 50.11 μ M. IC has the most inhibitory potential on TNF- α production when compared to NO. As a result, TNF- α was used in molecular docking.

2.3 *In silico* work

2.3.1 ADME computation

For isolated compound (IC), the estimated values of mol MW, QPlogPo/w, donorHB, and accptHB (Lipinski's rule) are all within the prescribed limits, showing that IC has drug-like quality [20]. SASA, FOSA, FISA, PISA, and volume of IC were computed to be 645.49, 456.87, 94.90, 93.66, and 1203.93, respectively. These measurements highlight the importance of solvent accessible surface area, as well as the hydrophobic, hydrophilic, and its π component required for interaction of IC with TNF- α . The values are within the given ranges, implying that IC is bound to the hydrophilic-hydrophobic contour of the TNF- α receptor. Oral absorption and percent oral absorption for humans and functional groups (reactive) have been calculated to be 3, 80.65, and 0 respectively. IC is likewise inactive in the CNS. Table 1 explains the significance of descriptors in further detail.

Table 1
Pharmacokinetic prediction of isolated compound (IC) by QikProp® 3.2

SI no.	Descriptor	Description	Recommended range	Predicted value of IC
1	mol_MW	Molecular weight of the molecule	130.0-725.0	387.48
2	SASA	Total solvent accessible surface area (SASA) in square angstroms using a probe with a 1.4 Å ⁰ radius	300.0-1000.0	645.49
3	FOSA	Hydrophobic component of the SASA (saturated carbon and attached hydrogen)	0.0-750.0	456.87
4	FISA	Hydrophilic component of the SASA (SASA on N, O and hydrogen on heteroatom)	7.0-330.0	94.90
5	PISA	Π (carbon and attached hydrogen) component of SASA	0.0-450.0	93.66
6	volume	Total solvent-accessible volume in cubic angstroms using a probe with 1.4 Å ⁰ radius	500.0-2000.0	1203.93
7	donorHB	Estimated number of hydrogen bonds that would be donated by the solute to water molecules in an aqueous solution. Values are averages taken over a number of configurations, so they can be non-integer	0.0-6.0	2.25
8	accptHB	Estimated number of hydrogen bonds that would be accepted by the solute to water molecules in an aqueous solution. Values are averages taken over a number of configurations, so they can be non-integer	2.0-20.0	7.25
9	QPlogP o/w	Predicted octanol / water partition coefficient	-2.0-6.5	1.992
10	Human oral absorption	Predictive qualitative human oral absorption. The assessment uses a knowledge-based set of rules, including checking for suitable values percent human oral absorption, number of metabolites, number of rotatable bonds logP, solubility and cell permeability	1, 2, 3 for low, medium and high absorption respectively	3
11	% human oral absorption	It predicts human oral absorption on 0 to 100% scale. The prediction is based on a quantitative multiple linear regression model. This property usually correlates well with human oral absorption.	>80% is high <25% is poor	80.65
12	#rtvFG	This particular descriptor indicates the number of reactive functional groups. The presence of these groups can lead to decomposition, reactivity, or toxicity problems <i>in vivo</i> .	0 to 2.0	0

Sl no.	Descriptor	Description	Recommended range	Predicted value of IC
13	CNS	Predictive central nervous activity on a -2 (inactive) to +2 (active) scale.	-2.0 to 2.0	0
14	Lipinski's rule of five	Lipinski's rules of five are: mol_MW < 500, QPlogPo/w < 5, donorHB ≤ 5, accptHB ≤ 10. Compounds that satisfy these rules are considered drug like. (The "five" refers to the limits, which are multiples of 5).	Maximum is 4	Satisfy the Lipinski's rule of five

2.3.2 Prediction of active site and molecular docking

With the amino acid residues **ASP 45** and **GLN 47**, IC forms two hydrogen bonds. (Figure 3) The oxy linkage of IC acts as a hydrogen bond acceptor in **GLN 47** and **ASP 45**, whereas the -NH of the pyrrolidine moiety acts as a hydrogen bond donor. The dock pose of IC, together with the hydrophilic-hydrophobic structure of the TNF- α receptor, yielded a G score of -5.36. (Figure 4).

2.4 In vivo experiment

2.4.1 Acute Toxicity Study

In male mice, the LD₅₀ doses of EE and IC were determined to be 3020 mg/kg b.w. and 2200 mg/kg b.w., respectively.

2.4.2 Effect of EE and IC on Carrageenan-produced oedema of paw in mice

A well-known and well-established paradigm for acute inflammation is carrageenan-induced inflammation. During the 4th and 5th hours after carrageenan therapy, oral doses of EE of 100 mg/kg and 200 mg/kg reduced inflammation in the same way. The percent inhibitory activities were 20.0 and 24.4 percent, respectively ($p < 0.05$), as compared to the control. At the 3rd, 4th, and 5th hours after receiving a 400 μ g/kg oral dose of IC, the percent inhibitions were 31.82, 35.56, and 33.33 percent, respectively ($p < 0.05$). At the same incubation time, percent inhibitions at 600 μ g/kg of IC were 36.36, 40.00, and 37.78 percent, respectively ($p < 0.05$). The percentage inhibitions were 38.64, 42.22, and 40.00 percent ($p < 0.05$) in the third, fourth, and fifth hours following aspirin therapy at an oral dosage of 10 mg/kg, respectively. The data showed that during the fourth hour after carrageenan therapy, the percent inhibition of IC at the aforementioned two doses and aspirin at a dose of 10mg/kg began to decrease. In the case of EE, however, the percent inhibition remains constant between the 4th and 5th hour (Figure 5).

2.4.3 Effect of EE and IC on xylene /arachidonic acid-produced oedema of ear

Inhibition of xylene-induced ear oedema inflammation by EE at 100 mg/kg and 200 mg/kg was 19.51 and 31.71 percent ($p < 0.05$), respectively. For the arachidonic acid-induced model, the inhibitions were 27.06 and 30.59 percent, respectively ($p < 0.05$). The suppression of xylene-induced ear oedema inflammation by IC at 400 and 600 $\mu\text{g}/\text{kg}$ was 50.00 and 53.66 percent, respectively ($p < 0.05$). The inhibitions were 48.24% and 52.944% for the arachidonic acid model, respectively ($p < 0.05$). The inhibitions of both models were 57.32 and 61.18 percent, respectively ($p < 0.05$), for aspirin at a dosage of 10 mg/kg (Figure 6).

3 Discussion

The project's purpose is to isolate a molecule, explain its structure, and research its mode of action of isolated compound (IC) through *in vitro*, *in silico*, and *in vivo* techniques. The isolated compound [(16-methoxy-10-(3-methylbutyl)-2-oxa-6, 9, 12-triaza-tricyclo [13.3.1.03, 7] nonadeca-1(18), 13, 15 (19), 16-tetraene-8, 11-Dione)] from the bark of *Zizyphus nummularia* has exhibited activity for the first time.

NO and PGE_2 are the main mediators produced by macrophages [21, 22]. According to research, TNF- α is an inflammatory cytokine that is thought to be an endogenous mediator in LPS-induced shock [23, 24]. The inflammatory response is boosted by excessive NO, PGE_2 , and TNF- α production, which destroys adjacent cells and tissues. As a result, any molecule that might lower these inflammatory mediators could be investigated as a potential anti-inflammatory chemical entity.

The molecular docking investigates the simulated environment required for IC and the expected TNF-receptor contact location. LYS 90, ASP 45, GLN 27, ARG 131, GLU 23, GLY 24, GLN 47, GLU 135, GLN 25, LEU 26, ASN 46 are among the amino acid residues found in the environment (Figure 7).

After demonstrating that IC has anti-inflammatory efficacy *in vitro* and that our *in-silico* work reflected the best possible understanding of IC's interactions with TNF- α , we put it to the test in a carrageenan-induced and xylene /arachidonic acid-produced inflammation model *in vivo*. The carrageenan test is one of the most sensitive tests available. In mice, it causes biphasic oedema [25]. This is due to an overabundance of inflammatory mediators such as nitric oxide and others. The findings revealed that IC generated more pronounced inhibition up to the fourth hour after carrageenan administration. Because of the existence of prostaglandins and the nature of sluggish reactions, the volume of oedema in the 3rd phase of oedema generated by carrageenan reaches a maximum [26]. Arachidonic acid modulates the production of nitric oxide as a secondary messenger [27]. It's also a PGE_2 precursor. As a result, the observed effect is caused by PGE_2 and/or NO production suppression. Pro-mediators of inflammation are released by sensory neurones from mast cells and other immune cells. This is made easier by xylene.

4. Conclusions

[(16-methoxy-10-(3-methyl-butyl)-2-oxa-6, 9, 12-triaza-tricyclo [13.3.1.03, 7] nonadeca-1(18), 13, 15 (19), 16-tetraene-8, 11-Dione)], a novel cyclic alkaloid compound (IC) isolated from the bark of the root of

Ziziphus nummularia, exhibited potential anti-inflammatory activity. In this study, IC significantly reduced the expression of inflammatory mediators such as NO and TNF- α . Carrageenan, xylene, and arachidonic acid-induced oedema were all significantly reduced by IC. Therefore, the compound may have clinical potential for the treatment of inflammation in future.

5. Materials And Methods / Experimental

5.1 Plant material

The root barks of *Ziziphus nummularia* were collected in the month of September 2010 from Durgapur, West Bengal, India (20°56' N, 84°53' E). The plant species was identified and authenticated by the Taxonomists of Botanical Survey of India, Shibpur, Howrah [Ref. no.:CNH/I-I/20/2010/Tech.II/171]. A voucher specimen (BCRCP/DP/PT/02/06) has been deposited in the Herbarium Dr. B. C. Roy College of Pharmacy & Allied Health Sciences, Durgapur, India for future reference.

5.2 Extraction, isolation & Identification

2.5 kg of powdered root barks were macerated in 5 litres of 70% (v/v) ethanol for one week (35 ± 5 °C) with intermittent shaking and stirring. Filters were used to remove particle matter and cellular debris from the extracts. Finally, the crude extract was concentrated in a rotary vacuum evaporator at low heat (< 40 °C) under reduced pressure to obtain semi-solid extract (55 g). As a result, the extract yield is 2.2 percent (w/w). The extract was kept in a desiccator to be used in continued study. 15.38g crude extract was combined with 32.14g of 60-120 mesh silica gel to make an admixture for isolation. Then a 2.4cm diameter column was packed with 30.05g of 60-120 mesh silica gel and 47.52g of Chloroform admixture. The column was then eluted with an increasing polarity solvent (chloroform to methanol). The isolated chemical yielded 0.075g (0.48 percent w/w).

Several fractions undergoing TLC analysis and plates sprayed with reagents for initial identification of phytoconstituents. The HPTLC analysis was done using CAMAG HPTLC. Melting point was measured and uncorrected. The ^1H NMR, ^{13}C NMR were done in Bruker 400 MHz instrument (Bruker, Germany). The IR spectrum was performed with KBr on FTIR-8400S (Shimadzu, Japan). Mass spectrum was on LC-MS/MS (API- 4000 TM, Applied BioSystems, MDS SCIEX, Canada). The high-resolution mass spectrum was on Thermo-Fisher Orbitrap Exploris 120 Mass Spectrometry (MS) system. Elemental analyses performed on a Perkin-Elmer (2400 Series II) analyzer (Perkin Elmer, USA).

5.3 Test Materials and Chemicals

The EE and IC utilised in the animal experiment were suspended in 1% tween-80 as a solvent. In this study, DMSO was used to solubilize IC in a master plate (resulting less than 0.4 percent DMSO concentration to avoid cytotoxicity in DMSO-producing cells). A variety of concentrated IC solutions in 100 percent DMSO were diluted in master plate (Briefly, a variety of concentrated IC solutions in (100

percent DMSO) were transferred in master plate. The dilution was then finished in a drug dilution plate (1:25 dilution ensuing 4 percent of DMSO). Finally, the cells received the desired concentration of IC solution (1:10 dilution producing 0.4 percent of DMSO).

RAW264.7 cell line was obtained from SIGMA-RBI, Switzerland. Dulbecco's Modified Eagle Medium (DMEM) both with and without phenol red, phosphate buffered saline (PBS) and Griess reagent was from Invitrogen (Carlsbad, USA). Lipopolysaccharide (LPS), foetal bovine serum (FBS) from *E. coli* serotype 0111: B4, interferon gamma (IFN γ) all were purchased from BD Biosciences (New Jersey, USA). The other reagents and chemicals were of HPLC grade.

5.4 *In vitro* inflammation inhibitory activity

5.4.1 Preparation of Cell culture and its stimulation

The RAW 264.7 murine monocytic macrophage cell line was maintained in DMEM supplemented with 10% FBS, 4.5 g/l glucose, sodium pyruvate (1 mM), L-glutamine (2 mM), streptomycin (50 μ g/ml), and penicillin (50 U/ml) at 37°C in the presence of 5% CO₂. Cells with a confluency of 80–90% were centrifuged at 120g for 10 minutes at 4°C to obtain a final cell concentration of 2 \times 10⁶ cells/ml. 50 μ L of cell suspension were placed to a 96-well tissue culture plate (4 \times 10⁵ cells/well). Then it was incubated at 37°C for 2 hours in the presence of 5% carbon dioxide. Following that, 100 U/ml IFN- γ and 5 μ g/ml LPS were given to the cells with / without the presence of the isolated compound (IC) evaluated, with a final volume of 100 μ L/well using DMSO as the vehicle. For the next 20 hours, the cells were incubated at 37°C in the presence of 5% carbon dioxide.

5.4.2 Estimation of NO, PGE₂, and TNF- α inhibitory activity of IC

Nitrite oxide was estimated by Griess reagent [28] as build-up of nitrite. It was quantified using sodium nitrite as a standard. PGE₂ and TNF- α in supernatant were estimated by ELISA kits (eBioscience, USA) as per manufacturer's instructions.

5.5 *In silico* ADME computation and molecular docking studies of IC

The ADME of the IC was calculated using an *in silico* method. Maestro Schrodinger (MS) programme [QikProp® (Version 3.2) module] created a pharmacokinetic outline of IC. At first IC was counterbalanced. Several descriptors including Lipinski's rule were calculated. The conformity of IC to Lipinski's rule indicates potential for molecule for future development.

5.5.1 Prediction of active site and molecular docking

The inflammation inhibition of IC on TNF- α was considered to explore exact form of inhibition of selected TNF- α receptor. Maestro 9.0 build panel was used for construction of 3D configurations of IC

(Schrödinger, LLC., USA). In this panel LigPrep 2.3 version was employed.

5.5.2 Preparation of the protein and prediction of active site

The protein was recombinant human TNF- α (resolution of 2.30 Å and crystal in nature) and was chosen from an available source (PDB ID: 1A8M) [29]. The Maestro Schrödinger®9.0 module was used to ground the structure as well as anticipate the active site. Because the selected TNF- α receptor lacked a correlated co-crystallized ligand, the exact location of the critical binding region on the receptor was unknown. As a result, the Sitemap® module (Maestro Schrödinger® 9.0, version v23118) was used to locate a promising binding hollow space within the receptor. Two binding sites were found in the output, and the binding site with the highest score (**0.643 in our case**) was chosen for molecular docking.

5.6 *In vivo* anti-inflammatory activity

The animal experiments performed as per ethical committee (Ref No: BCRCP/IAEC/8/2012). Albino mice (♂, 25±5 g, age: 2–3 months) kept inside standard polypropylene cages (3 mice/cage) at model laboratory environment of 12:12 light–dark cycle. The temperature as well as relative humidity was 20 ± 2°C and 55 ± 5% respectively.

5.6.1 Acute toxicity study

The work on acute toxicity for EE and IC performed as per method developed by Lorke [30]. The detail procedure was given in supplementary section (**Supplementary file: Material S1**)

5.6.2 Carrageenan produced oedema of paw in mice

Carrageenan-induced paw oedema in mice is a useful approach for evaluating the anti-inflammatory potential of active phytoconstituents [31]. Mice were starved for 12 hours before to the experiment. Sixty mice were divided into six groups (n=10). Group 1 received tween-80 (1%) orally, 30 minutes ahead of carrageenan injection. This group will act as inflammation control. Group 2 & 3 orally accepted 100 mg/kg & 200 mg/kg EE. Group 4 as well as 5 orally received 400 µg/kg and 600 µg/kg of IC. Group 6 given aspirin (10 mg /kg) and act as positive control. Following carrageenan administration, paw oedema was measured at 0 hour, 1 hour, 2 hours, 3 hours, 4 hours, and 5 hours.

5.6.3 Xylene /arachidonic acid-produced oedema of ear

For each model, mice were divided into six groups (n=10). Inflammation was generated in mice by applying 30 µl of following reagents (arachidonic acid 0.1 mg/µl in acetone [32] and xylene [33]) on inner & outer faces of right ear. Group 1 received tween-80 (1%) orally, 30 minutes ahead carrageenan injection. This group will act inflammation control. Group 2 & 3 orally accepted 100 mg/kg & 200 mg/kg EE. Group 4 and 5 orally received 400 µg/kg and 600 µg/kg of IC. Group 6 given aspirin (10 mg /kg) and act as positive control. Left ear acted normal control. All the mice sacrificed 30 minutes later arachidonic acid injection / xylene administration. The ears were taken away and weighed.

5.7 Statistical analysis

The result from the study showed in mean \pm S.E.M. The impact of the values is checked by student *t* test using computerized GraphPad InStat (version 3.05), GraphPad software, USA. Differences are measured significant when $p < 0.05$.

Declarations

Declaration of interest

The authors declare no conflict of interest.

Acknowledgement: The authors wish to thank Prof. Achintya Saha of Division of Pharmaceuticals & Fine chemicals, Department of Chemical Technology, University of Calcutta for providing computational support to carry out *in silico* experiment. One of the authors (SDR) also wishes to acknowledge the authority of Dr B C Roy College of Pharmacy & A.H.S for providing the necessary facility for carrying out the animal experiment.

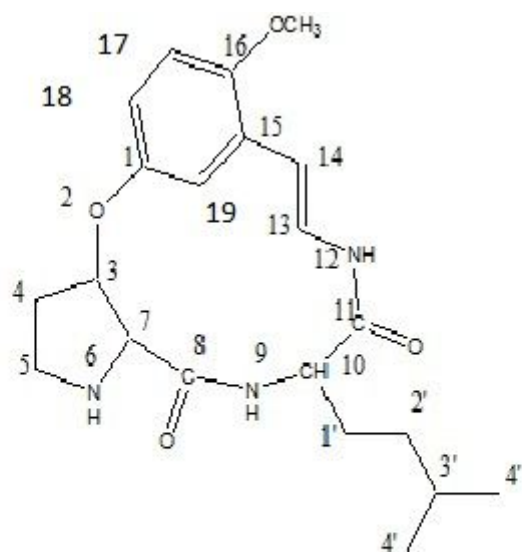
References

1. Cekici A, Kantarci A, Hasturk H, Van Dyke TE (2000) Inflammatory and immune pathways in the pathogenesis of periodontal disease. *Periodontol* 64(1):57–80. <https://doi.org/10.1111/prd.12002>
2. Siegfried G, Descarpentrie J, Evrard S, Khatib AM (2020) Proprotein convertases: Key players in inflammation-related malignancies and metastasis. *Cancer Lett* 473:50–61. <https://doi.org/10.1016/j.canlet.2019.12.027>
3. Qian BZ (2017) Inflammation fires up cancer metastasis. *Semin Cancer Biol* 47:170–176. <https://doi.org/10.1016/j.semcancer.2017.08.006>
4. Locati M, Curtale G, Mantovani A (2020) Diversity, Mechanisms, and Significance of Macrophage Plasticity. *Annu Rev Pathol* 15:123–147. <https://doi.org/10.1146/annurev-pathmechdis-012418-012718>
5. Davies LC, Taylor PR (2015) Tissue-resident macrophages: then and now. *Immunology* 144(4):541–548. <https://doi.org/10.1111/imm.12451>
6. Vignali DA, Kuchroo VK (2012) IL-12 family cytokines: immunological playmakers. *Nat Immun* 13(8):722–728. <https://doi.org/10.1038/ni.2366>
7. Montgomery SL, Bowers WJ (2012) Tumor necrosis factor-alpha and the roles it plays in homeostatic and degenerative processes within the central nervous system. *J Neuroimmune Pharmacol* 7(1):42–59. <https://doi.org/10.1007/s11481-011-9287-2>
8. Zelova H, Hosek J (2013) TNF- α signalling and inflammation: interactions between old acquaintances. *Inflamm Res* 62(7):641–651. <https://doi.org/10.1007/s00011-013-0633-0>
9. Habib S, Ali A (2011) Biochemistry of nitric oxide. *Indian J Clin Biochem* 26(1):3–17. <https://doi.org/10.1007/s12291-011-0108-4>

10. Allerton TD, Proctor DN, Stephens JM, Dugas TR, Spielmann G, Irving BA (2018) l-Citrulline Supplementation: Impact on Cardiometabolic Health. *Nutrients* 10(7):921–924. <https://doi.org/10.3390/nu10070921>
11. Ricciotti E, Fitzgerald GA (2011) Prostaglandins and inflammation. *Arterioscler Thromb Vasc Biol* 31(5):986–1000. <https://doi.org/10.1161/ATVBAHA.110.207449>
12. Biswas S, Shaw R, Bala S, Mazumdar A (2017) Inventorization of some ayurvedic plants and their ethnomedicinal use in Kakrajhore forest area of West Bengal. *J Ethnopharmacol* 197:231–241. <https://doi.org/10.1016/j.jep.2016.08.014>
13. Bachaya HA, Iqbal Z, Khan MN, Sindhu ZU, Jabbar A (2009) Anthelmintic activity of *Ziziphus nummularia* (bark) and *Acacia nilotica* (fruit) against Trichostrongylid nematodes of sheep. *J Ethnopharmacol* 123(2):325–329. <https://doi.org/10.1016/j.jep.2009.02.043>
14. Upadhyay B, Singh KP, Kumar A (2011) Ethno-veterinary uses and informants consensus factor of medicinal plants of Sariska region, Rajasthan, India. *J Ethnopharmacol* 133(1):14–25. <https://doi.org/10.1016/j.jep.2010.08.054>
15. Goyal M, Ghosh M, Nagori BP, Sasmal D (2013) Analgesic and anti-inflammatory studies of cyclopeptide alkaloid fraction of leaves of *Zizyphus nummularia*. *Saudi J Biol Sci* 20(4):365–371. <https://doi.org/10.1016/j.sjbs.2013.04.003>
16. Soliman YH (2011) Topical Anti-inflammatory and wound healing activities of herbal gel of *Ziziphus nummularia* L. (F. *Rhamnaceae*) leaf extract. *Int J Pharmacol* 7(8):862–867. <https://doi.org/10.3923/ijp.2011.862.867>
17. Goyal M, Sasmal D, Nagori BP (2012) Analgesic and anti-inflammatory activity of ethanolic extract of *Zizyphus nummularia*. *Res J Med Plant* 6:521–528. <https://doi.org/10.3923/rjmp.2012.521.528>
18. Dey Ray S, Dewanjee S (2015) Isolation of a new triterpene derivative and in vitro and in vivo anticancer activity of ethanolic extract from root bark of *Zizyphus nummularia* Aubrev. *Nat Prod Res* 29(16):1529–1536. <https://doi.org/10.1080/14786419.2014.983921>
19. Dey Ray S, Ray S, Zia-Ul-Haq M, De Feo V, Dewanjee S (2015) Pharmacological basis of the use of the root bark of *Zizyphus nummularia* Aubrev. (*Rhamnaceae*) as anti-inflammatory agent. *BMC Complement Altern Med* 15:416. <https://doi.org/10.1186/s12906-015-0942-7>
20. Lipinski CA, Lombardo F, Dominy BW, Feeney PJ (2001) Experimental and computational approaches to estimate solubility and permeability in drug discovery and development settings. *Adv Drug Deliv Rev* 46(1–3):3–26. [https://doi.org/10.1016/s0169-409x\(00\)00129-0](https://doi.org/10.1016/s0169-409x(00)00129-0)
21. Lin CY, Lee CH, Chang YW, Wang HM, Chen CY, Chen YH (2014) Pheophytin a inhibits inflammation via suppression of LPS-induced nitric oxide synthase-2, prostaglandin E2, and interleukin-1 β of macrophages. *Int J Mol Sci* 15(12):22819–22834. <https://doi.org/10.3390/ijms151222819>
22. Shi Q, Cao J, Fang L, Zhao H, Liu Z, Ran J, Zheng X, Li X, Zhou Y, Ge D, Zhang H, Wang L, Ran Y, Fu J (2014) Geniposide suppresses LPS-induced nitric oxide, PGE2 and inflammatory cytokine by downregulating NF- κ B, MAPK and AP-1 signaling pathways in macrophages. *Int Immunopharmacol* 20(2):298–306. <https://doi.org/10.1016/j.intimp.2014.04.004>

23. Ye H, Wang Y, Jenson AB, Yan J (2016) Identification of inflammatory factor TNF α inhibitor from medicinal herbs. *Exp Mol Pathol* 100(2):307–311. [https://doi.org/ 10.1016/j.yexmp.2015.12.014](https://doi.org/10.1016/j.yexmp.2015.12.014)
24. Parameswaran N, Patial S (2010) Tumor necrosis factor- α signaling in macrophages. *Crit Rev Eukaryot Gene Expr* 20(2):87–103. <https://doi.org/10.1615/critreveukargeneexpr.v20.i2.10>
25. Mukarram SM, Shah A (2015) Possible anti-inflammatory mechanism of ethyl acetate extracts of *Teucrium stocksianum* bioss. *BMC Complement Altern Med* 15:299. <https://doi.org/10.1186/s12906-015-0834-x>
26. Cong HH, Khaziakhmetova VN, Zigashina LE (2015) Rat paw oedema modelling and NSAIDs: Timing of effects. *Int J Risk Saf Med* 27:76–77. <https://doi.org/10.3233/JRS-150697>
27. Signorello MG, Segantin A, Leoncini G (2009) The arachidonic acid effect on platelet nitric oxide level. *Biochem Biophys Acta* 1791:1084–1092. [https://doi.org/ 10.1016/j.bbali.2009.07.003](https://doi.org/10.1016/j.bbali.2009.07.003)
28. Titheradge MA, Reed (1998) The enzymatic measurement of nitrate and nitrite. *Methods Mol Biol* 100:83–91. <https://doi.org/10.1385/1-59259-749-1:83>
29. Reed C, Fu ZQ, Wu J, Xue YN, Harrison RW, Chen MJ, Weber IT (1997) Crystal structure of TNF- α mutant R31D with greater affinity for receptor R1 compared with R2. *Protein Eng* 10(10):1101–1107. <https://doi.org/10.1093/protein/10.10.1101>
30. Lorke DA (1983) A new approach to practical acute toxicity testing. *Arch Toxicol* 54(4):275–287. [https://doi.org/ 10.1007/BF01234480](https://doi.org/10.1007/BF01234480)
31. Dordevic S, Petrovic S, Dobric S, Milenkovic M, Vucicevic D, Zizic S, Kukic J (2007) Antimicrobial, anti-inflammatory, anti-ulcer and antioxidant activities of *Carlina acanthifolia* root essential oil. *J Ethnopharmacol* 109(3):458–463. <https://doi.org/10.1016/j.jep.2006.08.021>
32. Young JM, Spires DA, Bedord CJ, Wagner B, Ballaron SJ, De Young LM (1984) The mouse ear inflammatory response to topical arachidonic acid. *J Invest Dermatol* 82(4):367–371. <https://doi.org/10.1111/1523-1747.ep12260709>
33. Nunez Guillen ME, Emim JA, Souccar C, Lapa AJ (1997) Analgesic and anti-inflammatory activities of the aqueous extract of *Plantago major* L. *Int J Pharmacogn* 35(2):99–104. <https://doi.org/10.1076/phbi.35.2.99.13288>

Figures



16-Methoxy-10-(3-methyl-butyl)-2-oxa-6,9,12-triaza-tricyclo[13.3.1.0^{3,7}]nonadeca-1(18),13,15(19),16-tetraene-8,11-dione

Figure 1

The structure and chemical name of the isolated compound (IC)

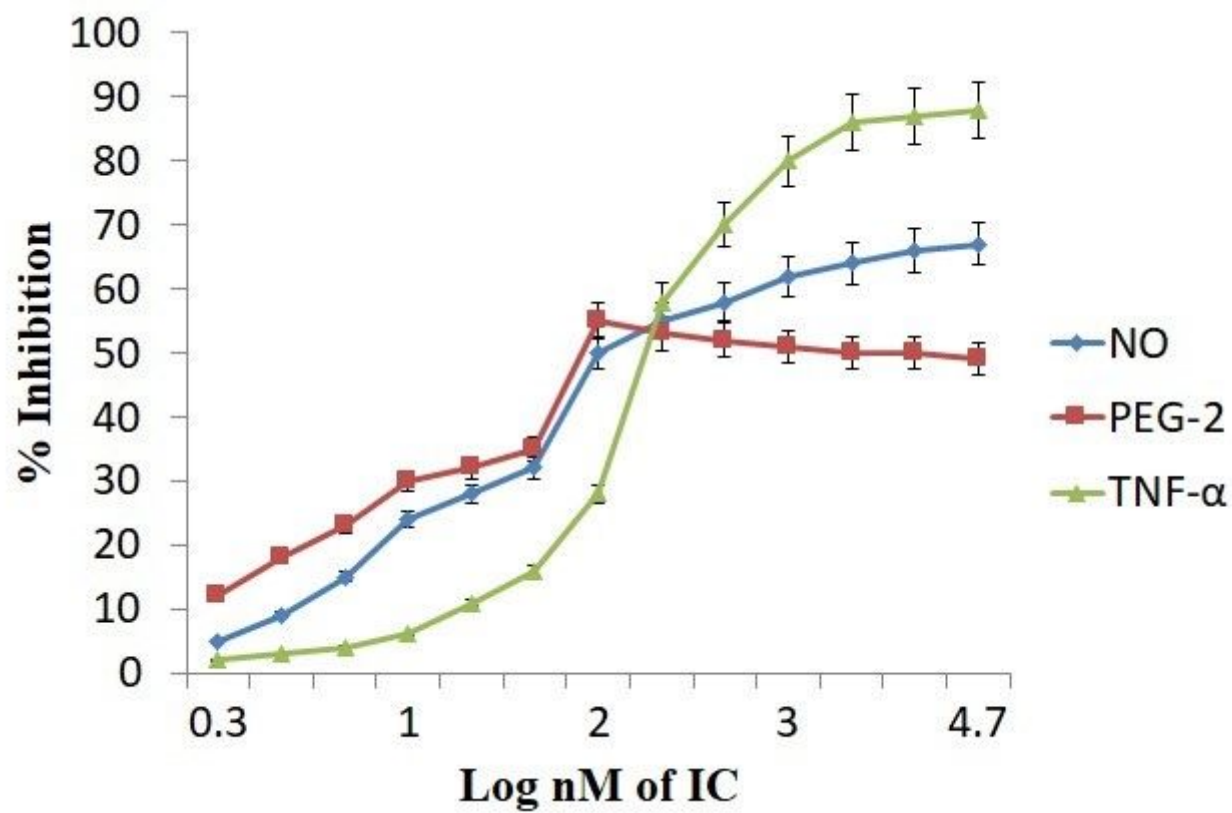


Figure 2

Effect of isolated compound (IC) on NO, PGE₂ and TNF- α production to demonstrate inflammatory inhibition potential

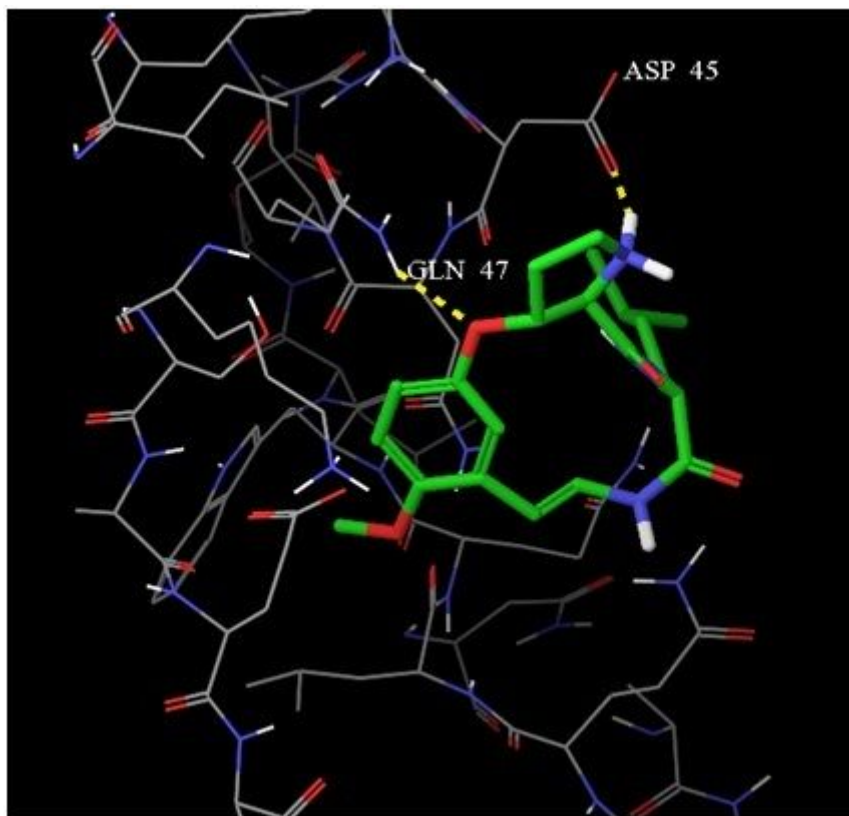


Figure 3

3D view of docking pose of minimum energy structure complex of isolated compound docked at the predicted active site of TNF alpha (PDB ID: 1A8M) viewed using Glide XP visualizer of Schrödinger Maestro. Hydrogen bonds are shown as yellow dash and bonded with ASP 45 and GLN 47

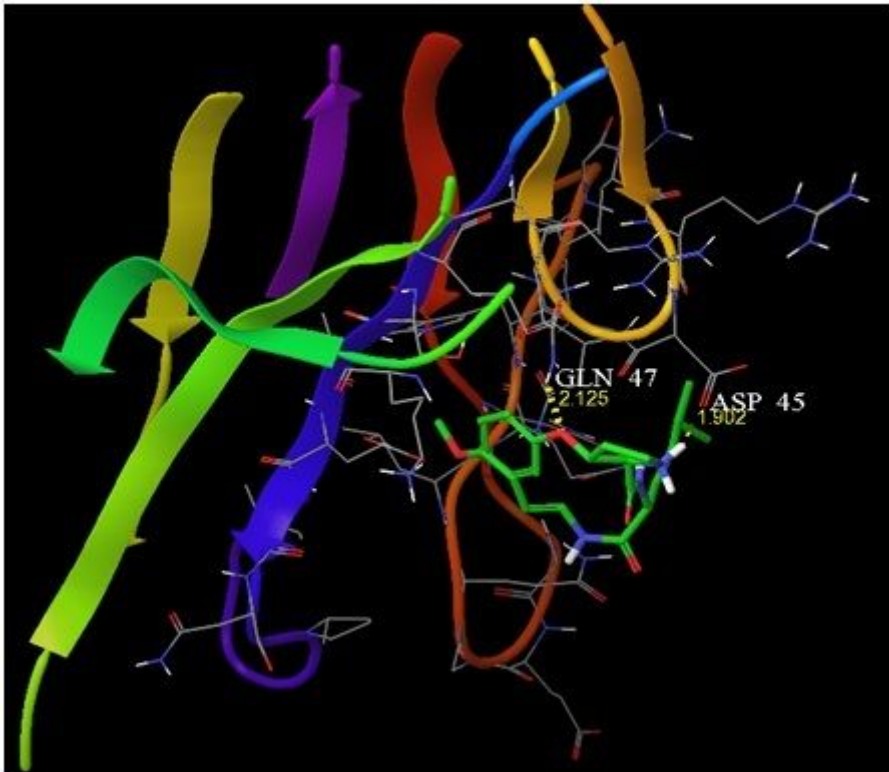


Figure 4

Dock pose of isolated compound (IC) complemented by the hydrophilic-hydrophobic shape of TNF- α receptor

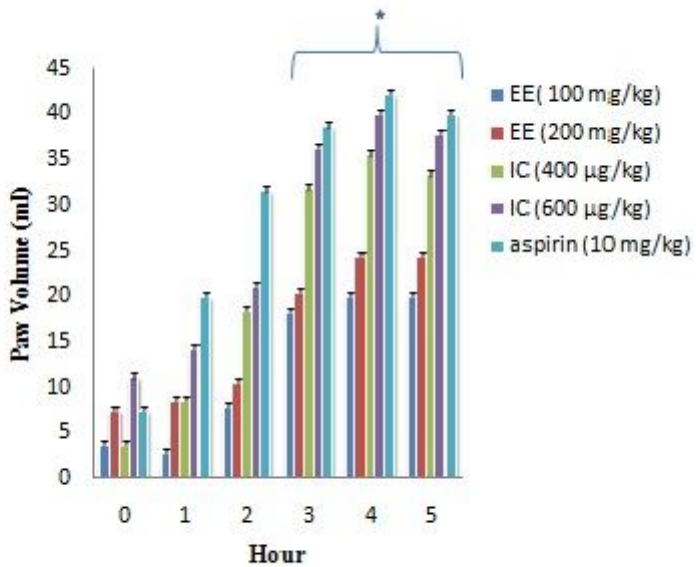


Figure 5

Effect of isolated compound (IC) and ethanolic extract (EE) on Carrageenan produced oedema of paw in mice (*p < 0.05 compared with control group)

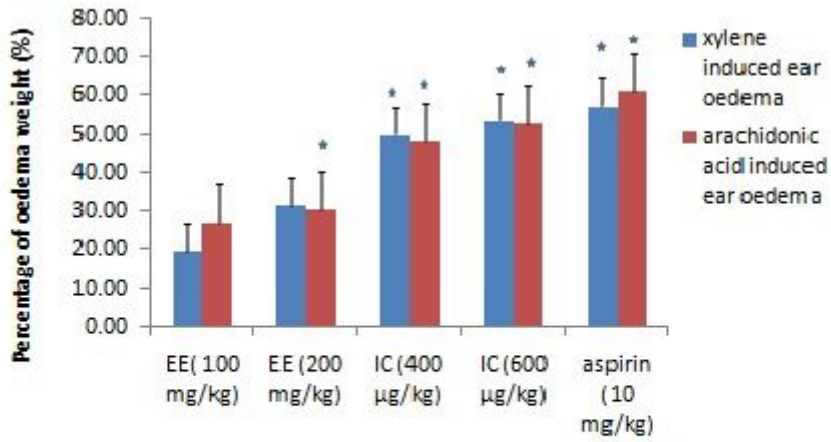


Figure 6

Effect of isolated compound (IC) and ethanolic extract (EE) on Xylene /arachidonic acid-produced oedema of ear (*p < 0.05 compared with control group)

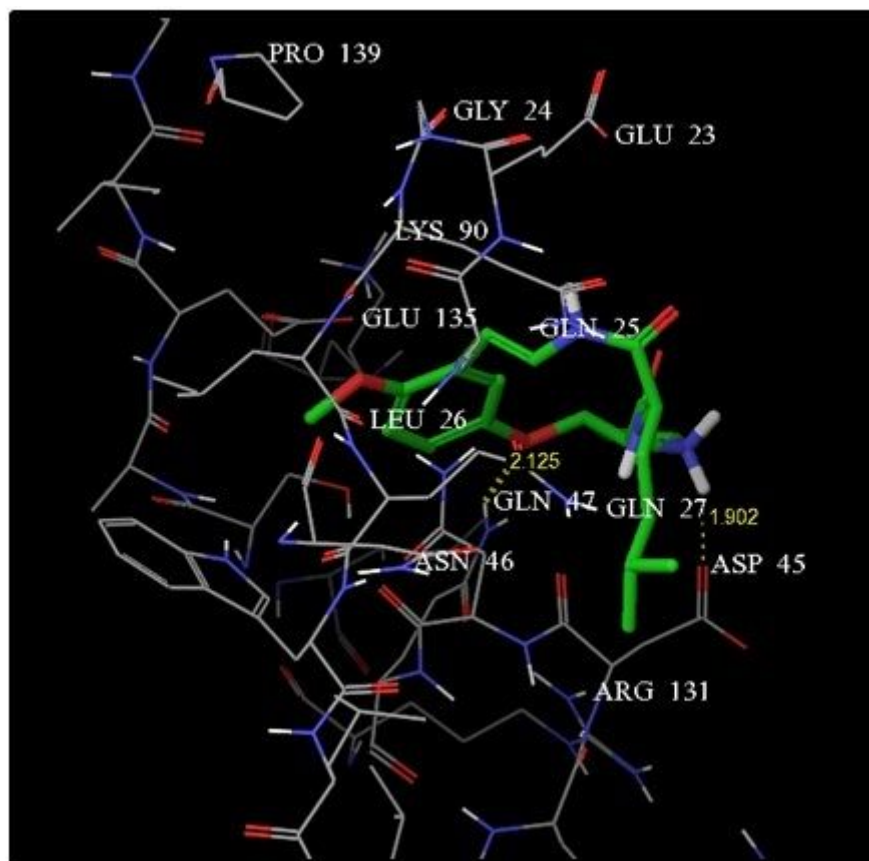


Figure 7

The key amino acid shown within the active site of TNF- α comprising LYS 90, ASP 45, GLN 27, ARG 131, GLU 23, GLY 24, GLN 47, GLU 135, GLN 25, LEU 26, ASN 46

Supplementary Files

This is a list of supplementary files associated with this preprint. Click to download.

- [FigureS1HPTLCprofiling.jpg](#)
- [FigureS21HNMRpageno1.jpg](#)
- [FigureS31HNMRpageno2.jpg](#)
- [FigureS41HNMRpageno3.jpg](#)
- [FigureS51HNMRpageno4.jpg](#)
- [FigureS613CNMR.jpg](#)
- [FigureS7FTIR.jpg](#)
- [FigureS8massspectra.jpg](#)
- [FigureS9HRMS.jpg](#)
- [MaterialS1.docx](#)